HHS Public Access

Author manuscript

Neurobiol Aging. Author manuscript; available in PMC 2017 July 01.

Published in final edited form as:

Neurobiol Aging. 2016 July ; 43: 79–88. doi:10.1016/j.neurobiolaging.2016.03.026.

Age-Dependent Differences in Brain Tissue Microstructure Assessed with Neurite Orientation Dispersion and Density Imaging

Andrew P. Merluzzi[1,2], **Douglas C. Dean III**[3], **Nagesh Adluru**[3], **Gaurav S. Suryawanshi**[3], **Ozioma C. Okonkwo**[1,8], **Jennifer M. Oh**[1], **Bruce P. Hermann**[8], **Mark A. Sager**[8], **Sanjay Asthana**[4,1], **Hui Zhang**[5], **Sterling C. Johnson**[4,1,8], **Andrew L. Alexander**[3,6,7], and **Barbara B. Bendlin**[1,8,*]

[1]Department of Medicine, Wisconsin Alzheimer's Disease Research Center, University of Wisconsin, Madison, Wisconsin

[2]Neuroscience and Public Policy Program, University of Wisconsin, Madison, Wisconsin

[3]Waisman Laboratory for Brain Imaging and Behavior, Madison, Wisconsin

Please address all correspondence to: Barbara B. Bendlin, Wisconsin Alzheimer's Disease Research Center, Department of Medicine, University of Wisconsin – Madison, Madison, WI 53705, Phone: (608) 265-2483, Fax: (608) 265-3091, ; Email: bbb@medicine.wisc.edu

7. DISCLOSURE STATEMENT

None of the authors have any conflicts of interest to declare. No author's institution has contracts relating to this research through which it or any other organization may stand to gain financially now or in the future. There are no other agreements of authors or their institutions that could be seen as involving a financial interest in this work.

Verification:

1. Disclosure
   a. None of the authors have any conflicts of interest to declare.
   b. No author's institution has contracts relating to this research through which it or any other organization may stand to gain financially now or in the future.
   c. There are no other agreements of authors or their institutions that could be seen as involving a financial interest in this work.
2. This project was supported by NIH grants R01AG037639 (BBB), AG027161 (SCJ), P50 AG033514 (SA), the Eunice Kennedy Shriver National Institute of Child Health and Human Development T32 HD007489 (DCD), the UW Institute for Clinical and Translation Research grant 1UL1RR025011, the Waisman Core Grant P30 HD003352-45, the Geriatric Research, Education, and Clinical Center (GRECC) of the William S. Middleton Memorial Veterans Hospital, and the National Science Foundation Graduate Research Fellowship under Grant No. DGE-1256259 (APM). Any opinions, findings, and conclusions or recommendations expressed in this material are those of the authors(s) and do not necessarily reflect the views of the National Science Foundation.
3. The data contained in this manuscript being submitted have not been previously published, have not been submitted elsewhere and will not be submitted elsewhere while under consideration at *Neurobiology of Aging*.
4. The University of Wisconsin's institutional review board approved all portions of this study and each subject provided written informed consent before all procedures.
5. All authors have reviewed the contents of the manuscript being submitted, approve of its contents and validate the accuracy of the data.

[4]Geriatric Research Education and Clinical Center, William S. Middleton Memorial Veteran's Hospital, Madison, Wisconsin

[5]Department of Computer Science & Centre for Medical Image Computing, University College London, UK

[6]Department of Medical Physics, University of Wisconsin School of Medicine and Public Health, Madison, Wisconsin

[7]Department of Psychiatry, University of Wisconsin School of Medicine and Public Health, Madison, Wisconsin

[8]Wisconsin Alzheimer's Institute

Abstract

Human aging is accompanied by progressive changes in executive function and memory, but the biological mechanisms underlying these phenomena are not fully understood. Using neurite orientation dispersion and density imaging (NODDI), we sought to examine the relationship between age, cellular microstructure, and neuropsychological scores in one hundred and sixteen late middle-aged, cognitively asymptomatic participants. Results revealed widespread increases in the volume fraction of isotropic diffusion (V_{iso}) and localized decreases in neurite density (NDI) in frontal white matter regions with increasing age. Additionally, several of these microstructural alterations were associated with poorer performance on tests of memory and executive function. These results suggest that NODDI is capable of measuring age-related brain changes and the neural correlates of poorer performance on tests of cognitive functioning, largely in accordance with published histological findings and brain-imaging studies of people of this age range. Ultimately, this study sheds light on the processes underlying normal brain development in adulthood, knowledge that is critical for differentiating healthy aging from changes associated with dementia.

Keywords

aging; diffusion-weighted imaging; MRI; neurites; cognition; microstructure

1. INTRODUCTION

Human aging involves progressive changes in neural architecture, including a loss of cortical dendritic spines, axonal alterations, and demyelination (Pannese, 2011). While gray matter (GM) changes – such as cortical thinning (Salat, et al., 2004) or reduced dendritic branching (Uylings and de Brabander, 2002) – have been well documented, white matter (WM) changes are also implicated in the aging process. Age-related changes have been observed in myelin (Aboitiz, et al., 1996), including a decline in the overall number and length of myelinated fibers (Marner, et al., 2003), as well as decreased myelin volume in older compared to younger participants (Tang, et al., 1997). These findings have been documented in post-mortem histological studies (as the three preceding references demonstrate) as well as in studies utilizing a common *in vivo* technique, diffusion-tensor imaging (DTI) (Salat, et al., 2005).

Diffusion-tensor imaging provides markers that include fractional anisotropy (FA) and mean diffusivity (MD), which serve as surrogates of tissue microstructure. The technique is sensitive to Brownian diffusion of water molecules, and microstructural features can be inferred given the relative coherence of myelinated axons in fiber tract bundles. Though DTI has proved invaluable for assessing changes in WM regions with age and determining the neural correlates of cognitive function (Madden, et al., 2004; Salat, et al., 2005; Charlton, et al., 2006; Sullivan and Pfefferbaum, 2006; Bendlin, et al., 2010; Nazeri, et al., 2015a), it is inherently a non-specific technique; a change in FA could reflect changes in myelination, axon diameter, axon packing density, or increased membrane permeability (Jones, et al., 2013). Further, DTI is insensitive to microstructural nuances within a particular voxel, such as regions in which WM tracts intersect, fan, or bend (Zhang, et al., 2012). This is particularly important given the abundance of crossing fibers in white matter (Jeurissen, et al., 2013). However, recent advances in diffusion-weighted imaging have allowed for a much closer inspection of cellular microstructure in humans.

One such technique is Hybrid Diffusion Imaging (HYDI) (Wu and Alexander, 2007) modeled with Neurite Orientation Dispersion and Density Imaging (NODDI) (Zhang, et al., 2012). HYDI acquires DTI and diffusion spectrum imaging (DSI) data simultaneously, allowing for collection of more diffusion directions and including higher b-values in a clinically reasonable scan time (Wu and Alexander, 2007;Zhang, et al., 2012). NODDI is capable of differentiating between three microstructural features: intra-neurite diffusion (within axons and dendrites), extra-neurite diffusion, and the volume fraction within a voxel occupied by isotropic water diffusion. It does this by modeling neurite orientation with a Watson distribution, which allows for a more accurate assessment of microstructure, including in regions with highly complex arborization such as in the cortex (Zhang, et al., 2012).

NODDI provides three parameters of interest: (1) neurite density index (NDI), which estimates the volume fraction within neurites and ranges in value from 0 (complete extra-neurite diffusion) to 1 (complete intra-neurite diffusion); (2) orientation dispersion index (ODI), which estimates the degree of fiber coherence, with values ranging from 0 (complete directional coherence) to 1 (fully dispersed neurites); and (3) volume within a voxel occupied by isotropic water diffusion (V_{iso}) similar to freely moving cerebrospinal fluid (CSF), with values from 0 (no CSF-like fluid) to 1 (complete CSF-like fluid). NODDI has been used to examine both normal brain development and disease conditions (Winston, et al., 2014; Lemkaddem, et al., 2014; Timmers, et al., 2015; Grussu, et al., 2015; Wen, et al., 2015; Figini, et al., 2014; Eaton-Rosen, et al., 2015; Kunz, et al., 2014; Jelescu, et al., 2015; Magnollay, et al., 2014; Adluru, et al., 2014; Billiet, et al., 2014; Stikov, et al., 2015). Such studies provide a more detailed analysis of the microstructural subtleties and underlying mechanisms associated with these illnesses and processes.

With regard to human aging, NODDI has been utilized in several studies investigating changes in WM and GM microstructure including a recent study by Nazeri, et al., 2015. In this analysis of forty-five cognitively healthy participants between 21 and 84 years, widespread decreases in ODI were observed with age throughout the cortex. This effect was particularly pronounced within frontoparietal regions, possibly indicating reduced dendritic

complexity or a regression of dendritic arborization (Nazeri, et al., 2015). Importantly, this result is largely in accordance with histological findings in monkeys (for a review, see Dickstein, et al., 2013) and humans showing age-related differences in dendritic complexity and density (Anderson and Rutledge, 1996). This group demonstrated no significant changes in NDI with age, possibly because analyses were limited to GM regions in which NDI values are lower than in WM (Zhang, et al., 2012). Several other studies have investigated age-related NODDI changes in WM in cohorts of healthy, relatively young individuals. One study, Billiet, et al., 2015, examined 59 participants (aged 17–70 years) and observed widespread cerebral V_{iso} increases in WM, as well as more localized NDI and ODI increases. Similarly, Chang, et al., 2015 observed increases in NDI and ODI in WM in a group of 66 healthy participants aged 7–63, though tending to over represent younger adults and therefore perhaps better modeling early-life development rather than aging through adulthood. Finally, Kodiweera, et al., 2015 used the HYDI acquisition protocol and examined changes specific to WM in 47 adults aged 18–55, finding increased ODI and no age-related changes in NDI. Perhaps most importantly, each of these studies found increases in ODI with increasing age, a microstructural phenomenon which may lend mechanistic insight into the increased FA seen in early development (Lebel and Beaulieu, 2011). By extension, Chang, et al., 2015 speculated that WM FA reductions often observed in older populations of participants may be due to either accelerated increases in ODI or slowing increases or reductions in NDI. There are known biological mechanisms to support this hypothesis, including the accumulation of water in myelin sheaths (Feldman and Peters, 1998), reduced packing density, or overall loss of myelinated fibers (Sandell and Peters, 2001; Marner, et al., 2003), and the present study may be able to shed light on this question by examining age-related differences in NDI and ODI in an older population.

While these prior studies provide important observations on age-related brain changes, each used relatively small sample sizes with wide age ranges, resulting in a sparse sampling across different ages. In the present study, we sought to determine the effect of age on NODDI metrics in a large sample of well-characterized middle- to older-aged adults. Given these previous studies and prior histological observations, we hypothesized: (1) age would be associated with a decrease in ODI and NDI in GM given potential age-related losses in neurite arborization; (2) ODI in WM would increase with age, reflecting greater dispersion of axons; (3) NDI would decrease with age in WM, reflecting reduced packing density; (4) V_{iso} would show age-dependent increases throughout the cerebrum, reflecting cell shrinkage with increasing age; (5) age-associated changes in NODDI measures would be observed within regions known to degenerate first in healthy aging, such as prefrontal WM (Reisberg, et al., 1999); and (6) greater age-associated changes in microstructure would be associated with lower memory and executive function.

2. METHODS

2.1 Participants

One hundred and sixteen cognitively healthy participants (mean age = 61.7; SD = 6.1; range 45.4–72.0; 62% female) were recruited from the Wisconsin Registry for Alzheimer's Prevention (WRAP) (Sager, et al., 2005) and the Wisconsin Alzheimer's Disease Research

Center (ADRC). The cohorts are composed of healthy middle to older-aged adults with and without parents with late onset AD. The current sample was enriched for AD risk via a parental history (72%) and included participants positive for the known AD genetic risk factor Apolipoprotein E ε4 (*APOE* ε4) (40%). Participants were defined as having a parental history of AD if one or both parents were determined to have the disease by a validated interview (Kawas, et al., 1994), or were confirmed AD positive by an autopsy reviewed by a multidisciplinary diagnostic consensus panel. Detailed medical history and phone interviews were conducted to confirm parental history negative participants. Absence of parental history of AD required that the participant's father survive to at least age 70 years and the mother to age 75 years without diagnosis of dementia or cognitive decline (McKhann, et al., 2011). Exclusion criteria included any significant neurological disease, MRI contraindications, major psychiatric disorders, or significant mental illness. While age was analyzed as a continuous variable, demographic characteristics and cognitive performance scores are listed in Table 1 by 3 age strata. The University of Wisconsin's institutional review board approved all portions of this study and each participant provided written informed consent before all procedures.

2.2 Neuropsychological Assessments

All participants underwent a comprehensive battery of cognitive tests administered by a trained psychometrist. For this study, we focused on the Rey Auditory Verbal Learning Test (RAVLT), and the Trail Making Test (TMT). Mini-mental state examination (MMSE) was used as a general screen (Folstein, et al., 1975). The RAVLT is a test of rote verbal learning and memory, which gauges participants' ability to recall 15 unrelated words over 5 trials and a later delayed recall. In this study, Trial 1 score was used to index immediate memory, trials 2–5 to index learning, and the delayed trial (20–30 minute delay) to assesses episodic memory recall (Schmidt, 1996; Lezak, 2004). The TMT, a test of simple (Part A) and complex (Part B) psychomotor tracking, involves drawing lines to connect objects as quickly as possible. Hence, more time to completion is indicative of poorer performance (Tombaugh, 2004; Ashendorf, et al., 2008). Part A requires participants to draw a line connecting sequential numbers, whereas Part B involves connecting alternating numbers and letters in sequence and is therefore more cognitively demanding. Scores from Part B were used in the current study as a measure of executive function.

2.3 Image Acquisition and Processing

Participants were imaged on a General Electric 3.0 Tesla MR750 scanner (Waukesha, WI) with an 8-channel head coil. Hybrid Diffusion Imaging (Wu and Alexander, 2007) was performed using a diffusion-weighted spin-echo echo-planar imaging pulse sequence with 132 DWI measurements spread across 6 q-space shells with the following b-values: 7 b=0, 6 b=300, 21 b=1200, 24 b=2700, 24 b=4800, and 50 b=7500 s/mm^2. The remaining parameters include δ = 37.8 ms and Δ = 43.1 ms, TR/TE=6500/102 ms, 96 × 96 matrix over 240 mm FOV with 3 mm thick slices (2.5×2.5×3.0 mm resolution). The total HYDI acquisition took approximately 15 minutes per participant for whole-brain, axial slice coverage. In addition to the diffusion-weighted images, the imaging protocol consisted of a 3D T1-weighted inversion recovery prepared fast spoiled gradient-echo image and a T2-weighted fluid attenuated inversion recovery (T2-FLAIR) image. 3D T1-weighted images

were acquired in the axial plane with the following parameters: inversion time (TI) = 450 ms; repetition time (TR) = 8.1 ms; echo time (TE) = 3.2 ms; NEX = 1; flip angle = 12°; acquisition matrix = 256 × 256 × 156; FOV = 256 mm; slice thickness = 1.0 mm, whereas 3D T2-weighted fluid attenuated inversion recovery (FLAIR) images were acquired in the sagittal plane using the following parameters: TI = 1869 ms; TR = 6000 ms; TE = 123 ms; flip angle = 90°; acquisition matrix = 256 × 256 × 100, FOV = 256 mm; slice thickness = 2.0 mm.

Upon acquisition, the DWI data were processed using the following procedures: First, images were converted from DICOM to NIFTI formats. All images were visually inspected for motion or distortion artifacts, but none were excluded on this basis. One participant was excluded due to an enlarged left ventricle; final n =116). Then, images were further assessed for motion-related artifacts using DTIPrep (https://www.nitrc.org/projects/dtiprep/), volumes deemed corrupted were removed, image distortions due to eddy currents were corrected using the "eddy" tool (Andersson and Sotiropoulos, 2016) as part of the FSL software package (http://fsl.fmrib.ox.ac.uk/fsl/fslwiki/), and diffusion gradients were reoriented using the output transformations from the eddy correction. Brain tissue was then extracted using FSL's Brain Extraction Tool (BET) (Smith, 2002), and tensor fitting was performed using the non-linear estimation tool in CAMINO (http://cmic.cs.ucl.ac.uk/camino/) for spatial normalization purposes. Finally, the diffusion-weighted images were fit using the NODDI Matlab toolbox (http://www.nitrc.org/projects/noddi_toolbox) extended to run in parallel on Condor (https://github.com/nadluru/NeuroImgMatlabCondor) to calculate the NODDI parameter maps. All parameter maps were visually inspected in three orthogonal views to assess signal dropout, distortion, or motion.

Following DTI and NODDI parameter map estimation, spatial normalization was performed in order to bring the participant data into a common analysis space. Non-linear diffeomorphic image registration of DTI data was implemented within the Diffusion Tensor Imaging ToolKit (DTI-TK; http://www.nitrc.org/projects/dtitk; Zhang, et al., 2006). Specifically, an iteratively optimized population-specific template was first created and the individual participant DTI data were non-linearly aligned to this template. DTI and NODDI parameter maps were brought into the population-specific template space by applying the affine and diffeomorphic transformations to the calculated parameter maps. Log-Euclidean interpolation was implemented, as this technique has been shown to preserve white matter orientation with minimal blurring (Arsigny, et al., 2006). To reduce potential partial volume effects, WM and GM masks were created. First, as has been done in previous studies (Nazeri, et al., 2015), each individual's FA map was segmented for WM using Atropos within the ANTS software package (Avants, et al., 2011). Next, each participant's composite image of WM and V_{iso} was subtracted from their whole-brain mask, creating a GM probability image (Nazeri, et al., 2015). Each individual's WM and GM images were then thresholded at a level of 0.7 to include only highly probable WM and GM voxels, respectively. Following this, aligned WM and GM masks were averaged across individuals and binarized. Each participant's NDI, ODI, and V_{iso} images were then smoothed at a 6mm FWHM Gaussian kernel within these tissue-specific population masks using 3dBlurInMask from the AFNI software package (Cox, 1996). For visualization purposes and to report coordinates in a standard space, an affine transformation between the population-specific

template and the Montreal Neurological Institute (MNI) template was calculated and applied to the resulting statistical maps using FSL (Jenkinson, et al., 2002).

White Matter Hyperintensity (WMH) due to presumed ischemia may confound interpretation of DWI results. As such, global WMH were used as an additional covariate in all statistical models presented here. White matter hyperintensity segmentation was achieved using the T1-weighted and T2-weighted images and the Lesion Segmentation Toolbox (LST) version 1.2.2 in SPM8 (http://www.fil.ion.ucl.ac.uk/spm/) (Schmidt, et al., 2012). Specifically, lesions were seeded based on spatial and intensity probabilities from T1-weighted images and hyperintense outliers on T2-FLAIR images, a method that has been validated with high agreement ($R^2 = 0.94$) to manual tracing (Schmidt, et al., 2012). When controlling for possible effects of WMH, global WMH was included in all statistical models as a ratio to intracranial volume (ICV). ICV was calculated using a "reverse brain masking" method (Keihaninejad, et al., 2010). Using segmentation procedures in SPM12, gray, white, and CSF International Consortium for Brain Mapping (ICBM) probability maps were created and then summed to produce an ICV probability map. Then, the inverse deformation field resulting from unified segmentation on each image was applied to the ICV probability map, in order to produce an ICV mask in native space. A threshold of 90% was applied to this participant-specific ICV probability map and the total volume was extracted. To control for variability in head size, the WMH variable was divided by ICV and multiplied by 100 to give a ratio (WMHr) in units of percent of ICV.

2.4 Statistical Analyses

Linear regressions with age as the predictor variable were performed in SPM12 separately on smoothed parameter maps in GM and WM, controlling for mean-centered, binary covariates of sex, parental history of AD, and *APOE* ε4 genotype. Additionally, regression analyses were run including the continuous variable of total brain WMHr burden as a covariate to determine if results were accounted for by ischemia. In all SPM12 analyses, significance was inferred at $\alpha < 0.05$ after FWE correction for multiple comparisons with an extent cluster size of 25 voxels to exclude small clusters and increase anatomical plausibility. Partial correlational analyses were run in SPSS to examine the relationship between the significant NODDI parameter clusters and neuropsychological scores, accounting for the effects of age, sex, *APOE* ε4 status, years of education, and parental history of AD. These correlations were also run with the continuous variable of total brain WMHr burden as an additional covariate. For all age-dependent effects on NODDI parameters, nonlinear least-squares regression was used to determine if a quadratic function (with age squared as the independent variable) produced a statistically larger R^2 value than ordinary least squares regression. Finally, to test if cognitive scores differed in individuals at risk for AD, we performed independent-samples t-tests between the groups of *APOE* ε4 positive versus negative, as well as between the groups of parental history positive versus negative.

2.5 Cognitive Scores

While all participants were non-demented, a range of cognitive performance was evident. The mean, SD (in parentheses), and range of each cognitive test were as follows: MMSE: 29.3 (1.0), 25–30; TMT-B: 59.0 (20.2), 28–125; RAVLT Immediate: 6.7 (1.9), 1–13; RAVLT

Learning: 45.3 (7.1), 23–59; RAVLT Delayed: 10.8 (3.1), 0–15. Two participants performed poorly on TMT-B, and therefore analyses examining TMT-B were run both including and excluding these two participants. Finally, three participants had MMSE scores between 25–26, while the remaining 113 participants had scores ≥ 27. Importantly, the three participants with lower MMSE scores did not score outside of 2.0 SD on the other cognitive tests, suggesting that no particular individual demonstrated cognitive functioning outside the normal range. Corroborating this, there were no significant differences on any cognitive test between individuals at risk for AD (via *APOE* ε4 positivity or parental history of AD) and those without increased risk (all p's > 0.05). Across all participants, the average time between neuropsychological testing and the MRI scan was 110 days (SD = 128 days), ranging from 0 to 491 days.

3. RESULTS

3.1 Brain Imaging Metrics

Representative NDI, ODI, V_{iso}, FA, and MD images from one participant are displayed in Figure 1. Age was associated with NODDI measurements. Figure 2 illustrates scatterplots from four NDI WM clusters reduced with increasing age. Figure 3 illustrates these findings in MNI brain space for reduced NDI in WM (panel A) and increased V_{iso} in GM (panel B). Table 2 details all significant clusters and statistics for NDI results. Overall, we observed decreases in NDI with advancing age in frontal WM regions, including the ventromedial and dorsomedial frontal cortex, the left anterior internal capsule, posterior to the medial frontal gyrus, and a superior frontal region anterior to the premotor cortex. We also observed widespread increases in V_{iso} throughout several cortical regions, particularly localized to the WM/GM border regions within frontal, parietal, and temporal lobes. Age was also significantly associated with WMHr (Pearson's Correlation = 0.264, p = 0.004), however the relationships between age and the NODDI maps were unchanged by the addition of WMHr as a covariate. Additionally, no relationships between age and NODDI metrics were modeled more accurately for quadratic rather than linear regressions (all p-values > 0.05 for R^2 changes). No significant findings were observed for ODI in either GM or WM, no significant results were observed for NDI in GM, and no significant results were observed for V_{iso} in WM.

3.2 Relationships Between Imaging Metrics and Cognitive Scores

Cognitive function was associated with NODDI measurements after accounting for age, sex, parental history of AD, years of education, and *APOE* ε4 genotype. Partial correlations revealed that lower NDI in left frontal superior WM was associated with poorer performance on the learning portion of the RAVLT; lower NDI in right frontal superior WM was associated with poorer performance on the trail-making test (TMT) part B (excluding two participants scoring poorly on this test); lower NDI in left frontal inferior WM was associated with poorer performance on the learning portion of the RAVLT; and finally lower NDI in right frontal inferior WM was associated with poorer performance on the learning portion of the RAVLT (all p's < 0.05; scatterplots shown in Figure 4). When accounting for WMHr burden, only the effects of right frontal inferior NDI on RAVLT learning and right frontal superior NDI on TMT-B remained significant, suggesting that WMHr accounted for

a significant portion of the variance in the two remaining associations. No significant relationships were found for scores on the RAVLT delayed test.

4. DISCUSSION

Age is associated with both gross and microscopic brain changes, and new advances in *in vivo* imaging are improving the ability to map these changes across the life span. This cross-sectional study investigated the extent to which age is associated with changes in NDI, ODI, and V_{iso} in GM and WM. Our results reveal that increasing age predicts higher V_{iso} near WM/GM border regions within sulci of the cortex, in the interhemispheric fissure, and in subcortical regions including adjacent to the bilateral hippocampus. By contrast, decreases in NDI were localized to frontal WM regions, suggesting that some regional increases in V_{iso} may reflect cell shrinkage without accompanying neurite density changes or, by extension, cell loss. In contrast, ODI was not influenced by age.

In general, the findings of the present study provide some replication of previous studies examining NODDI and healthy aging, in addition to providing contrasting findings. In a previous study of 59 adults aged 17–70 years, widespread increases in V_{iso} were observed throughout most of the cerebrum, similar to the results presented here (Billiet, et al., 2015). This finding suggests widespread increases in extracellular water with age, possibly reflecting cell shrinkage or changes in axon or myelin structure. Importantly, the fact that our V_{iso} findings are in accordance with the previous study – which used a much wider age range and younger cohort than the current study – suggests that the microstructural changes underlying the increase in V_{iso} between ages 17–70 also likely occur between ages 45–72. Furthermore, these results coincide with volumetric findings showing that both cortical (Fjell, et al., 2009) and hippocampal (Fjell, et al., 2009a) volumes decline with age, and additionally that hippocampal volumes exhibit an accelerated loss of volume beginning approximately at age 60 (Fjell, et al., 2013; for a review see Fjell, et al., 2014).

As such, it is especially interesting that greater water diffusion was present in bilateral hippocampus with increasing age. More specifically, we observed increased V_{iso} in anterior regions of CA3, CA1, and the dentate gyrus. Perhaps most importantly, a similar increase in V_{iso} was not observed in the entorhinal cortices, regions that are most associated with cell death in AD (Mueller, et al., 2010; Mueller and Weiner, 2009; for a review, see Small, et al., 2011). Volumetric studies have shown a relative preservation of the entorhinal cortices in healthy aging, and age-related shrinkage localized to CA1, CA3, and the dentate gyrus (Shing, et al., 2011). As with all MRI-based studies, these results should be interpreted with caution given the known limits in image resolution. This may be especially true of the diffusion-weighted data presented here, which contains voxel sizes larger than might typically be acquired in diffusion-weighted sequences. With this caveat in mind, the hippocampal findings do suggest that the results are representative of healthy aging, despite the fact that this sample is enriched with a parental history of AD.

With respect to NDI, our findings deviate from Billiet, et al., 2015 and Chang, et al., 2015. Whereas these studies observed increases in NDI with age in various WM regions, we observed decreases in frontal WM, including the ventromedial and dorsomedial prefrontal

cortex. This discrepancy may best be reconciled by comparing the age ranges of the participant pools. The relative lack of older participants in the prior studies may have obscured changes that occur later in life, whereas the current study likely lacks sensitivity for changes that occur earlier in development. Importantly, the participant pools in both Billiet, et al., 2015 and the current study may lack the necessary age range to detect nonlinear changes in WM, a finding that has emerged in previous research using NODDI (Chang, et al., 2015) and other techniques (Allen, et al., 2005; Jernigan and Gamst, 2005; Walhovd, et al., 2011; Fjell, et al., 2013). For instance, one previous study using DTI in 77 healthy adults (aged 19–84; mean = 56.49; SD = 16.80) revealed that age-related differences in WM diffusivity were typically best modeled by quadratic functions, with younger and older participants showing higher diffusivity than persons of middle age (~55 years old) in most brain regions (Kennedy and Raz, 2009). Moreover, other work has demonstrated positive correlations between cerebral WM volume and age until approximately 60 years, with strong negative correlations thereafter (Fjell, et al., 2013; Westlye, et al., 2009). Ultimately, more studies with age ranges beginning early in life and continuing into the 8th and 9th decade will be needed to determine if NODDI parameters are similarly sensitive to nonlinear trends in brain development, as results from previous studies have suggested. Regardless, our NDI results are largely in agreement with the anterior-posterior gradient observed in aging and the retrogenesis hypothesis, or the “last in, first out” model in which fibers that myelinate latest in development tend to be the first to degenerate with age (Brickman, et al., 2012; Fjell, et al., 2009; Reisberg, et al., 1999; Head, et al., 2004).

Billiet, et al., 2015, Kodiweera, et al., 2015, and Chang, et al., 2015 also observed ODI increases with age, suggesting that fibers disperse, fan, or bend away from each other with advancing age. Our results do not replicate this, again perhaps due to differences in age between the populations or the more stringent multiple comparison correction requisite for a whole-brain analysis. Indeed, uncorrected data ($p<0.001$) from our sample demonstrate some age-dependent WM ODI increases in similar regions as in the previous studies (data not shown). However, it should be noted that widespread *decreases* in orientation dispersion were also observed with age at this uncorrected threshold, making interpretation difficult. Moreover, these increases and decreases in ODI did not localize to GM or WM specifically or in a way consistent with our hypotheses, further complicating interpretation. One technical reason that we failed to observe changes in ODI may be due to the HYDI acquisition protocol. Specifically, HYDI emphasizes the sampling of many different b-values, thereby reducing the density of orientation sampling within any particular b-value. However, the ODI images analyzed here are visually comparable to those presented elsewhere with 2- and 4-shell procedures (Zhang, et al., 2012), and HYDI has been used to estimate ODI with success previously (Kodiweera, et al., 2015). While we do not exclude the possibility that utilizing fewer b-values while sampling many directions would result in significant ODI results in the current study, this seems unlikely. Further research is needed to resolve these hypotheses, specifically comparing 2-, 4-, and 6-shell diffusion-weighted acquisitions. Still, the fact that we observed the most robust decreases in NDI in frontal WM regions *without* corresponding increases in ODI (taking into account the aforementioned acquisition caveat) does coincide with the hypothesis that the decreases in FA often reported in older populations may be due to decreased NDI rather than increased ODI (Chang, et al.,

2015). This is further supported by the fact that the most robust decreases in FA in our sample are spatially aligned to two significant regions in which increasing age is associated with reduced NDI in frontal dorsomedial WM (FA data not shown).

Another study that examined NODDI and healthy aging looked exclusively in GM (Nazeri, et al., 2015). In this study, widespread decreases in cerebral GM ODI were observed with advancing age. This finding is not unexpected, as age-related decreases in dendritic branching, spine density, and complexity have been observed in histological studies as discussed previously (Dickstein, et al., 2013). In this context, it is somewhat surprising that our results do not replicate the same pattern of ODI decreases in cerebral GM. However, as with the NDI findings, this discrepancy may be accounted for by the difference in age range between the two participant groups. By 45 years of age (the youngest participant in our cohort) or 61 years of age (the mean age) it may be that the greatest age-related decreases in dendritic branching or spine density have already occurred, thereby preventing us from detecting any further age-related differences in the ODI measure. Corroborating this hypothesis, previous neuron tracing findings from 10 healthy adult males (21–71 years old) revealed that while individuals above 55 years of age had greatly reduced dendritic lengths and spine densities in supragranular pyramidal cells compared to individuals younger than 55, dendritic length and spine density did not statistically differ within participants older than 55 (Anderson and Rutledge, 1996). If ODI is indeed sensitive to changes in dendritic complexity, our results suggest that after the 5th or 6th decade of life, dendritic microstructure remains stable in healthy aging. If replicated, this finding may have important implications for detecting and separating nascent neurodegeneration from healthy aging relatively early in life.

With respect to cognitive function, we observed that reduced NDI in dmPFC and vmPFC WM predicted poorer performance on the RAVLT learning test and TMT-B. The role of the vmPFC in cognition is well established, and these results with NODDI parameters are in agreement with those showing that reductions in vmPFC volume or PFC lesions correlate with worse performance on tests of executive function, memory encoding, and memory retrieval (Gunning-Dixon and Raz, 2003; Blumenfeld and Ranganath, 2007; Alexander, et al., 2007). Importantly, adding WMHr burden as an additional covariate accounted for the association between left vmPFC and dmPFC on RAVLT learning, suggesting that vascular brain health at least partially mediates these relationships. This finding corroborates previous studies, which have shown that WMH tend to accumulate with age, localize in frontal WM regions, and are associated with deficits in processing speed, immediate and delayed memory, as well as executive function (Gunning-Dixon and Raz, 2000; Raz, et al., 2003; Raz, et al., 2007). Importantly, while we limited examination to only two tests from a much larger neuropsychological battery and only used significant NDI clusters in the frontal WM, these findings are unlikely to survive correction for multiple comparisons, particularly with a stringent correction method such as Bonferroni. As such, these results should be interpreted with caution and warrant replication in future studies. Still, the neuropsychological findings presented here may demonstrate an early link between microstructural alterations and cognitive impairment independent of risk for AD in a clinically healthy population.

There are limitations in the current study which merit discussion. First, as previously mentioned, our cohort of asymptomatic individuals was enriched for Alzheimer's disease risk. In an attempt to account for this fact, we statistically controlled for parental history of AD and *APOE* ε4 genotype in all analyses, and the covariates of *APOE* ε4 genotype, parental history of AD, or their interactions with age were not significant in regressions predicting the NODDI parameters or cognitive scores. Furthermore, there were no differences between individuals at risk versus those not at risk on any cognitive measure, as previously mentioned. Regardless, our interpretations of these findings as representative of "healthy aging" are done cautiously. Second, as with all cross-sectional designs, these results do not represent "aging" so much as "age-dependent differences," which could possibly be accounted for by cohort effects. For instance, it is possible that the older individuals participating in our study are healthier than average for this age cohort, thereby biasing our sample. However, if this were the case, we would likely be underestimating effect sizes, both for pathology in the brain and for lower scores on neuropsychological tests. Ultimately, longitudinal designs utilizing NODDI are required to truly understand how NDI, V_{iso}, and ODI vary as individuals age through adulthood. And despite our deliberate attempts to create tissue-specific masks, all diffusion-weighted imaging studies must be interpreted while considering that registration, interpolation, or partial volume effects may account for significant findings. Similarly, methodological differences between studies (including skeletonization of WM and GM, as has been done in previous studies examining NODDI in aging) must also be taken into account when comparing across studies. More generally, NODDI metrics will need further validation particularly with respect to the cellular changes that underlie increased V_{iso}; while some change in tissue must likely account for increased space for CSF to diffuse, this could be due to axonal degeneration, demyelination, dendritic alterations, or some other microstructural alteration. Interestingly, in this sample of participants widespread age-related increases in MD in GM were observed. However, in contrast to the V_{iso} findings, no MD results survived corrections for multiple comparisons. This possibly indicates that the V_{iso} metric from the NODDI protocol is more sensitive to microstructural changes than MD from traditional DTI, even if increases in V_{iso} merely represent early signs of age-related atrophy. It is possible that future research using markers in CSF of axon, myelin, or dendrite degeneration would further aid in understanding the nature of age-related microstructural changes and V_{iso}. Additionally, multimodal imaging sensitive to different tissue types in the same participants and from the same MRI scanning session will be invaluable for understanding how tissue structure changes across the spectrum of aging.

5. CONCLUSION

NODDI provides a new measure for assessing brain changes in aging, differentiating between microstructural features that were previously undefined with conventional DTI, including NDI, ODI, and V_{iso}. Older age was associated with greater V_{iso} across widespread GM, and NDI decreases were observed in localized frontal WM regions, findings that were independent of ischemic injury. In contrast, ODI was unaffected by age in this cohort. Ultimately, more sophisticated modeling of water diffusion is expected to inform trajectories of brain and cognitive aging.

Acknowledgments

This project was supported by NIH grants R01AG037639 (BBB), AG027161 (SCJ), P50 AG033514 (SA), the Eunice Kennedy Shriver National Institute of Child Health and Human Development T32 HD007489 (DCD), the UW Institute for Clinical and Translation Research grant 1UL1RR025011, the Waisman Core Grant P30 HD003352-45, the Geriatric Research, Education, and Clinical Center (GRECC) of the William S. Middleton Memorial Veterans Hospital, and the National Science Foundation Graduate Research Fellowship under Grant No. DGE-1256259 (APM). Any opinions, findings, and conclusions or recommendations expressed in this material are those of the authors(s) and do not necessarily reflect the views of the National Science Foundation. The authors acknowledge the support of researchers and staff at the Waisman Center and the Wisconsin Institute for Medical Research at the University of Wisconsin-Madison, where imaging data were collected. Finally, the authors thank their dedicated participants for their valuable time.

ABBREVIATIONS

DTI	Diffusion Tensor Imaging
PIB	Pittsburgh compound B
WRAP	Wisconsin Registry for Alzheimer's Prevention
FA	fractional anisotropy
MD	mean diffusivity
APOE4	apolipoprotein E gene ε4
FH	(parental) family history
WM	white matter
GM	gray matter
SPM	Statistical Parametric Mapping
FSL	FMRIB Software Library
BET	Brain Extraction Tool
DTI-TK	Diffusion Tensor Imaging Toolkit
RAVLT	Rey Auditory Verbal Learning Test
TMT	Trail Making Test
FWE	family wise error
ANTS	Advanced Normalization Tools
dmPFC	dorsomedial prefrontal cortex
vmPFC	ventromedial prefrontal cortex
AFNI	Analysis of Functional Neuroimages

References

Aboitiz F, Rodriquez E, Olivares R, Zaidel E. Age-related changes in the fibre composition of the human corpus callosum: sex differences. NeuroReport. 1996; 7(11):1761–4. [PubMed: 8905659]

Adluru, G.; Gur, Y.; Anderson, JS.; Richards, LG.; Adluru, N.; DiBella, EV. Assessment of white matter microstructure in stroke patients using NODDI. Engineering in Medicine and Biology Society (EMBC), 2014 36th Annual International Conference of the IEEE; IEEE; 2014. p. 742-5.

Alexander MP, Stuss DT, Picton T, Shallice T, Gillingham S. Regional frontal injuries cause distinct impairments in cognitive control. Neurology. 2007; 68(18):1515–23. [PubMed: 17470755]

Allen JS, Bruss J, Brown CK, Damasio H. Normal neuroanatomical variation due to age: the major lobes and a parcellation of the temporal region. Neurobiol Aging. 2005; 26(9):1245–60. discussion 79–82. DOI: 10.1016/j.neurobiolaging.2005.05.023 [PubMed: 16046030]

Anderson B, Rutledge V. Age and hemisphere effects on dendritic structure. Brain. 1996; 119:1983–90. [PubMed: 9010002]

Andersson JL, Sotiropoulos SN. An integrated approach to correction for off-resonance effects and subject movement in diffusion MR imaging. NeuroImage. 2016; 125:1063–78. [PubMed: 26481672]

Arsigny V, Fillard P, Pennec X, Ayache N. Log-Euclidean metrics for fast and simple calculus on diffusion tensors. Magnetic resonance in medicine. 2006; 56(2):411–21. [PubMed: 16788917]

Ashendorf L, Jefferson AL, O'Connor MK, Chaisson C, Green RC, Stern RA. Trail Making Test errors in normal aging, mild cognitive impairment, and dementia. Archives of Clinical Neuropsychology. 2008; 23(2):129–37. [PubMed: 18178372]

Avants BB, Tustison NJ, Wu J, Cook PA, Gee JC. An open source multivariate framework for n-tissue segmentation with evaluation on public data. Neuroinformatics. 2011; 9(4):381–400. [PubMed: 21373993]

Bendlin BB, Fitzgerald ME, Ries ML, Xu G, Kastman EK, Thiel BW, Rowley HA, Lazar M, Alexander AL, Johnson SC. White matter in aging and cognition: a cross-sectional study of microstructure in adults aged eighteen to eighty-three. Dev Neuropsychol. 2010; 35(3):257–77. DOI: 10.1080/87565641003696775 [PubMed: 20446132]

Billiet T, Deprez S, Maedler B, Peeters R, Zhang H, Leemans A, Dhollander T, Christiaens D, Amant F, Smeets A. Investigating the long-term effects of systemic chemotherapy on brain white matter using multi-shell diffusion MRI and myelin water imaging. Proc Intl Soc Mag Reson Med. 2014:1915.

Billiet T, Vandenbulcke M, Madler B, Peeters R, Dhollander T, Zhang H, Deprez S, Van den Bergh BR, Sunaert S, Emsell L. Age-related microstructural differences quantified using myelin water imaging and advanced diffusion MRI. Neurobiol Aging. 2015; 36(6):2107–21. DOI: 10.1016/j.neurobiolaging.2015.02.029 [PubMed: 25840837]

Blumenfeld RS, Ranganath C. Prefrontal cortex and long-term memory encoding: an integrative review of findings from neuropsychology and neuroimaging. The Neuroscientist. 2007; 13(3):280–91. [PubMed: 17519370]

Brickman AM, Meier IB, Korgaonkar MS, Provenzano FA, Grieve SM, Siedlecki KL, Wasserman BT, Williams LM, Zimmerman ME. Testing the white matter retrogenesis hypothesis of cognitive aging. Neurobiology of aging. 2012; 33(8):1699–715. [PubMed: 21783280]

Chang YS, Owen JP, Pojman NJ, Thieu T, Bukshpun P, Wakahiro ML, Berman JI, Roberts TP, Nagarajan SS, Sherr EH. White Matter Changes of Neurite Density and Fiber Orientation Dispersion during Human Brain Maturation. PloS one. 2015; 10(6):e0123656. [PubMed: 26115451]

Charlton R, Barrick T, McIntyre D, Shen Y, O'Sullivan M, Howe F, Clark C, Morris R, Markus H. White matter damage on diffusion tensor imaging correlates with age-related cognitive decline. Neurology. 2006; 66(2):217–22. [PubMed: 16434657]

Cox RW. AFNI: software for analysis and visualization of functional magnetic resonance neuroimages. Computers and Biomedical research. 1996; 29(3):162–73. [PubMed: 8812068]

Dickstein DL, Weaver CM, Luebke JI, Hof PR. Dendritic spine changes associated with normal aging. Neuroscience. 2013; 251:21–32. DOI: 10.1016/j.neuroscience.2012.09.077 [PubMed: 23069756]

Eaton-Rosen Z, Melbourne A, Orasanu E, Cardoso MJ, Modat M, Bainbridge A, Kendall GS, Robertson NJ, Marlow N, Ourselin S. Longitudinal measurement of the developing grey matter in preterm subjects using multi-modal MRI. NeuroImage. 2015; 111:580–9. [PubMed: 25681570]

Feldman ML, Peters A. Ballooning of myelin sheaths in normally aged macaques. Journal of neurocytology. 1998; 27(8):605–14. [PubMed: 10405027]

Figini M, Baselli G, Riva M, Bello L, Zhang H, Bizzi A. NODDI performs better than DTI in brain tumors with vasogenic edema. Proc Intl Soc Mag Reson Med. 2014:0271.

Fjell AM, McEvoy L, Holland D, Dale AM, Walhovd KB. AsDN Initiative. What is normal in normal aging? Effects of aging, amyloid and Alzheimer's disease on the cerebral cortex and the hippocampus. Progress in neurobiology. 2014; 117:20–40. [PubMed: 24548606]

Fjell AM, Walhovd KB, Fennema-Notestine C, McEvoy LK, Hagler DJ, Holland D, Brewer JB, Dale AM. One-year brain atrophy evident in healthy aging. The Journal of Neuroscience. 2009a; 29(48):15223–31. [PubMed: 19955375]

Fjell AM, Westlye LT, Amlien I, Espeseth T, Reinvang I, Raz N, Agartz I, Salat DH, Greve DN, Fischl B, Dale AM, Walhovd KB. High consistency of regional cortical thinning in aging across multiple samples. Cereb Cortex. 2009; 19(9):2001–12. DOI: 10.1093/cercor/bhn232 [PubMed: 19150922]

Fjell AM, Westlye LT, Grydeland H, Amlien I, Espeseth T, Reinvang I, Raz N, Holland D, Dale AM, Walhovd KB. Critical ages in the life course of the adult brain: nonlinear subcortical aging. Neurobiology of aging. 2013; 34(10):2239–47. [PubMed: 23643484]

Folstein MF, Folstein SE, McHugh PR. "Mini-mental state": a practical method for grading the cognitive state of patients for the clinician. Journal of psychiatric research. 1975; 12(3):189–98. [PubMed: 1202204]

Grussu F, Schneider T, Zhang H, Alexander DC, Wheeler–Kingshott CA. Neurite orientation dispersion and density imaging of the healthy cervical spinal cord in vivo. NeuroImage. 2015; 111:590–601. [PubMed: 25652391]

Gunning-Dixon FM, Raz N. The cognitive correlates of white matter abnormalities in normal aging: a quantitative review. Neuropsychology. 2000; 14(2):224. [PubMed: 10791862]

Gunning-Dixon FM, Raz N. Neuroanatomical correlates of selected executive functions in middle-aged and older adults: a prospective MRI study. Neuropsychologia. 2003; 41(14):1929–41. [PubMed: 14572526]

Head D, Buckner RL, Shimony JS, Williams LE, Akbudak E, Conturo TE, McAvoy M, Morris JC, Snyder AZ. Differential vulnerability of anterior white matter in nondemented aging with minimal acceleration in dementia of the Alzheimer type: evidence from diffusion tensor imaging. Cerebral Cortex. 2004; 14(4):410–23. [PubMed: 15028645]

Jelescu IO, Veraart J, Adisetiyo V, Milla SS, Novikov DS, Fieremans E. One diffusion acquisition and different white matter models: How does microstructure change in human early development based on WMTI and NODDI? NeuroImage. 2015; 107:242–56. [PubMed: 25498427]

Jenkinson M, Bannister P, Brady M, Smith S. Improved optimization for the robust and accurate linear registration and motion correction of brain images. Neuroimage. 2002; 17(2):825–41. [PubMed: 12377157]

Jernigan TL, Gamst AC. Changes in volume with age--consistency and interpretation of observed effects. Neurobiol Aging. 2005; 26(9):1271–4. discussion 5–8. DOI: 10.1016/j.neurobiolaging.2005.05.016 [PubMed: 16006011]

Jeurissen B, Leemans A, Tournier JD, Jones DK, Sijbers J. Investigating the prevalence of complex fiber configurations in white matter tissue with diffusion magnetic resonance imaging. Human brain mapping. 2013; 34(11):2747–66. [PubMed: 22611035]

Jones DK, Knösche TR, Turner R. White matter integrity, fiber count, and other fallacies: the do's and don'ts of diffusion MRI. Neuroimage. 2013; 73:239–54. [PubMed: 22846632]

Kawas C, Segal J, Stewart WF, Corrada M, Thal LJ. A validation study of the Dementia Questionnaire. Archives of Neurology. 1994; 51(9):901–6. [PubMed: 8080390]

Keihaninejad S, Heckemann RA, Fagiolo G, Symms MR, Hajnal JV, Hammers A. AsDN Initiative. A robust method to estimate the intracranial volume across MRI field strengths (1. 5 T and 3T). Neuroimage. 2010; 50(4):1427–37. [PubMed: 20114082]

Kennedy KM, Raz N. Pattern of normal age-related regional differences in white matter microstructure is modified by vascular risk. Brain Res. 2009; 1297:41–56. DOI: 10.1016/j.brainres.2009.08.058 [PubMed: 19712671]

Kodiweera C, Alexander AL, Harezlak J, McAllister TW, Wu Y-C. Age effects and sex differences in human brain white matter of young to middle-aged adults: A DTI, NODDI, and q-space study. NeuroImage. 2015

Kunz N, Zhang H, Vasung L, O'Brien KR, Assaf Y, Lazeyras F, Alexander DC, Hüppi PS. Assessing white matter microstructure of the newborn with multi-shell diffusion MRI and biophysical compartment models. Neuroimage. 2014; 96:288–99. [PubMed: 24680870]

Lebel C, Beaulieu C. Longitudinal development of human brain wiring continues from childhood into adulthood. The Journal of Neuroscience. 2011; 31(30):10937–47. [PubMed: 21795544]

Lemkaddem A, Daducci A, Kunz N, Lazeyras F, Seeck M, Thiran J-P, Vulliémoz S. Connectivity and tissue microstructural alterations in right and left temporal lobe epilepsy revealed by diffusion spectrum imaging. NeuroImage: Clinical. 2014; 5:349–58. [PubMed: 26236626]

Lezak, MD. Neuropsychological assessment. Oxford university press; 2004.

Madden DJ, Whiting WL, Huettel SA, White LE, MacFall JR, Provenzale JM. Diffusion tensor imaging of adult age differences in cerebral white matter: relation to response time. Neuroimage. 2004; 21(3):1174–81. DOI: 10.1016/j.neuroimage.2003.11.004 [PubMed: 15006684]

Magnollay L, Grussu F, Wheeler-Kingshott CA, Sethi V, Zhang H, Chard D, Miller DH, Ciccarelli O. An investigation of brain neurite density and dispersion in multiple sclerosis using single shell diffusion imaging. brain. 2014; 61:1000–16.

Marner L, Nyengaard JR, Tang Y, Pakkenberg B. Marked loss of myelinated nerve fibers in the human brain with age. J Comp Neurol. 2003; 462(2):144–52. DOI: 10.1002/cne.10714 [PubMed: 12794739]

McKhann GM, Knopman DS, Chertkow H, Hyman BT, Jack CR, Kawas CH, Klunk WE, Koroshetz WJ, Manly JJ, Mayeux R. The diagnosis of dementia due to Alzheimer's disease: Recommendations from the National Institute on Aging-Alzheimer's Association workgroups on diagnostic guidelines for Alzheimer's disease. Alzheimer's & Dementia. 2011; 7(3):263–9.

Mueller SG, Schuff N, Yaffe K, Madison C, Miller B, Weiner MW. Hippocampal atrophy patterns in mild cognitive impairment and Alzheimer's disease. Human brain mapping. 2010; 31(9):1339–47. [PubMed: 20839293]

Mueller SG, Weiner MW. Selective effect of age, Apo e4, and Alzheimer's disease on hippocampal subfields. Hippocampus. 2009; 19(6):558–64. [PubMed: 19405132]

Nazeri A, Chakravarty MM, Rajji TK, Felsky D, Rotenberg DJ, Mason M, Xu LN, Lobaugh NJ, Mulsant BH, Voineskos AN. Superficial white matter as a novel substrate of age-related cognitive decline. Neurobiol Aging. 2015a; 36(6):2094–106. DOI: 10.1016/j.neurobiolaging.2015.02.022 [PubMed: 25834938]

Nazeri A, Chakravarty MM, Rotenberg DJ, Rajji TK, Rathi Y, Michailovich OV, Voineskos AN. Functional Consequences of Neurite Orientation Dispersion and Density in Humans across the Adult Lifespan. The Journal of Neuroscience. 2015; 35(4):1753–62. [PubMed: 25632148]

Pannese E. Morphological changes in nerve cells during normal aging. Brain Structure & Function. 2011; 216(2):85–9. DOI: 10.1007/s00429-011-0308-y [PubMed: 21431333]

Raz N, Rodrigue KM, Acker JD. Hypertension and the brain: vulnerability of the prefrontal regions and executive functions. Behavioral neuroscience. 2003; 117(6):1169. [PubMed: 14674838]

Raz N, Rodrigue KM, Kennedy KM, Acker JD. Vascular health and longitudinal changes in brain and cognition in middle-aged and older adults. Neuropsychology. 2007; 21(2):149. [PubMed: 17402815]

Reisberg B, Franssen EH, Hasan SM, Monteiro I, Boksay I, Souren LE, Kenowsky S, Auer SR, Elahi S, Kluger A. Retrogenesis: clinical, physiologic, and pathologic mechanisms in brain aging, Alzheimer's and other dementing processes. European Archives of Psychiatry and Clinical Neuroscience. 1999; 249(3):S28–S36.

Sager MA, Hermann B, La Rue A. Middle-aged children of persons with Alzheimer's disease: APOE genotypes and cognitive function in the Wisconsin Registry for Alzheimer's Prevention. Journal of geriatric psychiatry and neurology. 2005; 18(4):245–9. [PubMed: 16306248]

Salat DH, Buckner RL, Snyder AZ, Greve DN, Desikan RS, Busa E, Morris JC, Dale AM, Fischl B. Thinning of the cerebral cortex in aging. Cereb Cortex. 2004; 14(7):721–30. DOI: 10.1093/cercor/bhh032 [PubMed: 15054051]

Salat DH, Tuch DS, Greve DN, van der Kouwe AJ, Hevelone ND, Zaleta AK, Rosen BR, Fischl B, Corkin S, Rosas HD, Dale AM. Age-related alterations in white matter microstructure measured by diffusion tensor imaging. Neurobiol Aging. 2005; 26(8):1215–27. DOI: 10.1016/j.neurobiolaging.2004.09.017 [PubMed: 15917106]

Sandell JH, Peters A. Effects of age on nerve fibers in the rhesus monkey optic nerve. Journal of Comparative Neurology. 2001; 429(4):541–53. [PubMed: 11135234]

Schmidt, M. Rey auditory verbal learning test: a handbook. Western Psychological Services; Los Angeles: 1996.

Schmidt P, Gaser C, Arsic M, Buck D, Förschler A, Berthele A, Hoshi M, Ilg R, Schmid VJ, Zimmer C. An automated tool for detection of FLAIR-hyperintense white-matter lesions in multiple sclerosis. Neuroimage. 2012; 59(4):3774–83. [PubMed: 22119648]

Shing YL, Rodrigue KM, Kennedy KM, Fandakova Y, Bodammer N, Werkle-Bergner M, Lindenberger U, Raz N. Hippocampal subfield volumes: age, vascular risk, and correlation with associative memory. Frontiers in aging neuroscience. 2011; 3

Small SA, Schobel SA, Buxton RB, Witter MP, Barnes CA. A pathophysiological framework of hippocampal dysfunction in ageing and disease. Nature Reviews Neuroscience. 2011; 12(10):585–601. [PubMed: 21897434]

Smith SM. Fast robust automated brain extraction. Human brain mapping. 2002; 17(3):143–55. [PubMed: 12391568]

Stikov N, Campbell JS, Stroh T, Lavelée M, Frey S, Novek J, Nuara S, Ho M-K, Bedell BJ, Dougherty RF. In vivo histology of the myelin g-ratio with magnetic resonance imaging. NeuroImage. 2015

Sullivan EV, Pfefferbaum A. Diffusion tensor imaging and aging. Neurosci Biobehav Rev. 2006; 30(6):749–61. DOI: 10.1016/j.neubiorev.2006.06.002 [PubMed: 16887187]

Tang Y, Nyengaard J, Pakkenberg B, Gundersen H. Age-induced white matter changes in the human brain: a stereological investigation. Neurobiology of aging. 1997; 18(6):609–15. [PubMed: 9461058]

Timmers I, Zhang H, Bastiani M, Jansma BM, Roebroeck A, Rubio-Gozalbo ME. White matter microstructure pathology in classic galactosemia revealed by neurite orientation dispersion and density imaging. Journal of inherited metabolic disease. 2015; 38(2):295–304. [PubMed: 25344151]

Tombaugh TN. Trail Making Test A and B: normative data stratified by age and education. Archives of clinical neuropsychology. 2004; 19(2):203–14. [PubMed: 15010086]

Uylings HBM, de Brabander JM. Neuronal Changes in Normal Human Aging and Alzheimer's Disease. Brain and Cognition. 2002; 49(3):268–76. DOI: 10.1006/brcg.2001.1500 [PubMed: 12139954]

Walhovd KB, Westlye LT, Amlien I, Espeseth T, Reinvang I, Raz N, Agartz I, Salat DH, Greve DN, Fischl B, Dale AM, Fjell AM. Consistent neuroanatomical age-related volume differences across multiple samples. Neurobiol Aging. 2011; 32(5):916–32. DOI: 10.1016/j.neurobiolaging.2009.05.013 [PubMed: 19570593]

Wen Q, Kelley DA, Banerjee S, Lupo JM, Chang SM, Xu D, Hess CP, Nelson SJ. Clinically feasible NODDI characterization of glioma using multiband EPI at 7T. NeuroImage: Clinical. 2015

Westlye LT, Walhovd KB, Dale AM, Bjørnerud A, Due-Tønnessen P, Engvig A, Grydeland H, Tamnes CK, Østby Y, Fjell AM. Life-span changes of the human brain white matter: diffusion tensor imaging (DTI) and volumetry. Cerebral cortex. 2009:bhp280.

Winston GP, Micallef C, Symms MR, Alexander DC, Duncan JS, Zhang H. Advanced diffusion imaging sequences could aid assessing patients with focal cortical dysplasia and epilepsy. Epilepsy research. 2014; 108(2):336–9. [PubMed: 24315018]

Wu Y-C, Alexander AL. Hybrid diffusion imaging. NeuroImage. 2007; 36(3):617–29. [PubMed: 17481920]

Zhang H, Schneider T, Wheeler-Kingshott CA, Alexander DC. NODDI: practical in vivo neurite orientation dispersion and density imaging of the human brain. Neuroimage. 2012; 61(4):1000–16. [PubMed: 22484410]

Zhang H, Yushkevich PA, Alexander DC, Gee JC. Deformable registration of diffusion tensor MR images with explicit orientation optimization. Medical image analysis. 2006; 10(5):764–85. [PubMed: 16899392]

Highlights

- Age is correlated with decreased neurite density in frontal lobe white matter
- Age is correlated with increased isotropic water diffusion throughout the brain
- Age-related brain changes are associated with cognitive functioning
- These results shed light on the brain processes underlying normal human aging

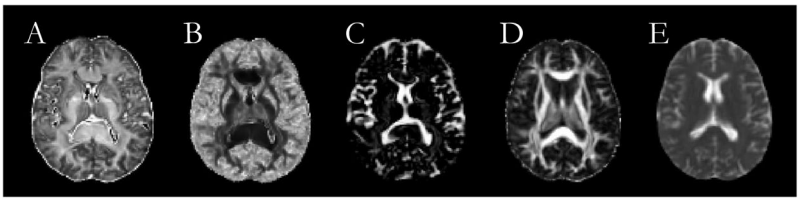

Figure 1.

Shown here are representative brain maps from one participant. Neurite density (panel A), orientation dispersion (panel B), isotropic volume fraction (panel C), fractional anisotropy (panel D), and mean diffusivity (panel E) are displayed.

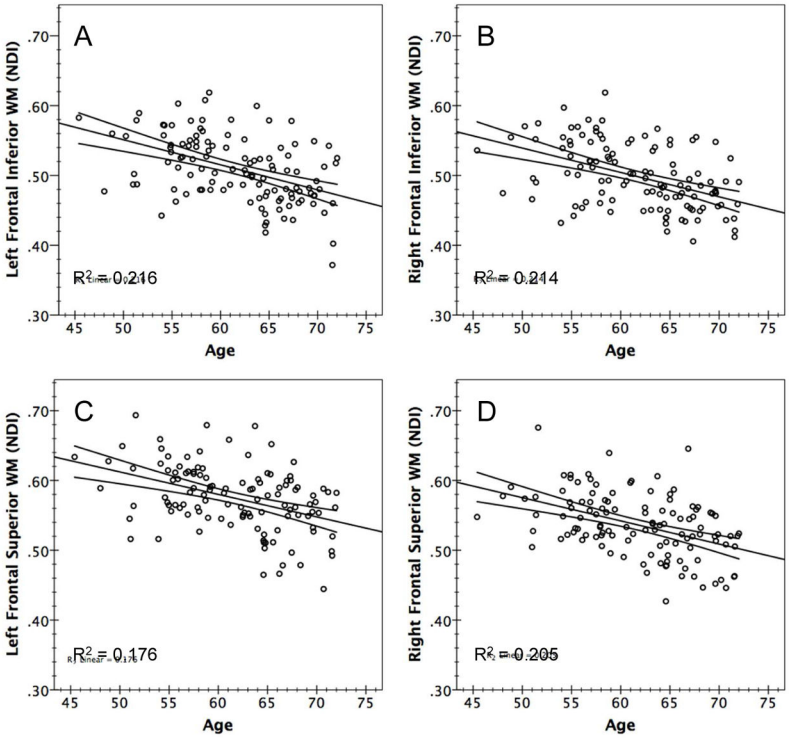

Figure 2.

Shown here is the relationship between age (in years) and neurite density (NDI) in four white matter regions in the frontal cortex, including bilateral ventromedial and dorsomedial frontal cortex. In all cases, age is negatively associated with neurite density, accounting for sex, *APOE* ε4 genotype, and parental history of AD.

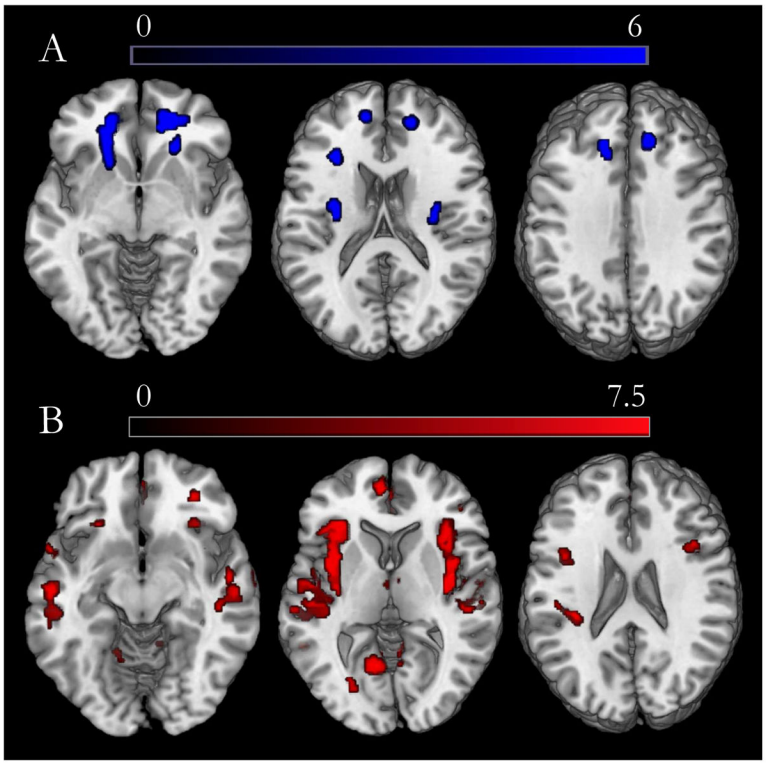

Figure 3.

Axial view brain maps with highlighted regions in which neurite density (NDI) decreases with increasing age in WM (panel A) and regions in which the volume fraction of isotropic diffusion (V_{iso}) increases with increasing age in GM (panel B). All images are presented in neurological convention (left on the left), and results are family-wise error corrected with a threshold of $p < 0.05$. The color bars represent the size of the t-statistic, with blue representing decreased NDI and red representing increased V_{iso}.

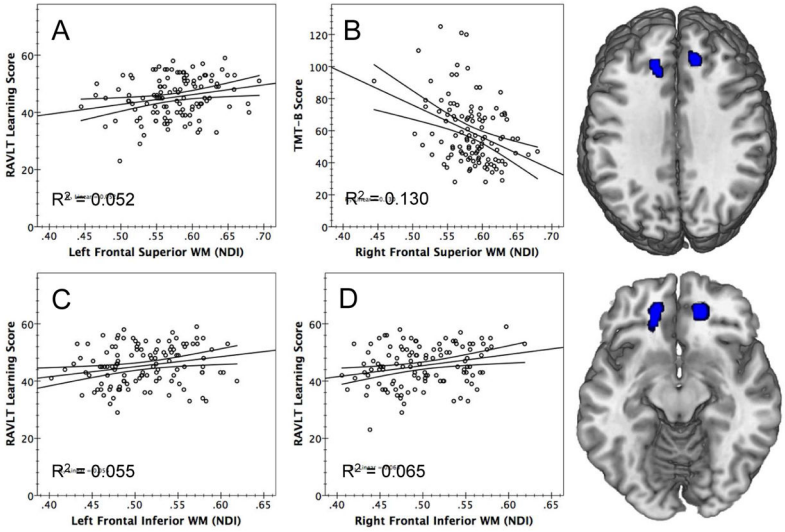

Figure 4.

Panel A: Lower neurite density (NDI) in left frontal superior white matter (WM) is associated with poorer performance on the learning portion of the Rey Auditory Verbal Learning Test (RAVLT). Panel B: Lower NDI in right frontal superior WM is associated with poorer performance on the trail-making test (TMT) part B (this scatterplot excludes two participants who scored poorly on this test; n=114). Panel C: Lower NDI in left frontal inferior WM is associated with poorer performance on the learning portion of the RAVLT. Panel D: Lower NDI in right frontal inferior WM is associated with poorer performance on the learning portion of the RAVLT. Corresponding statistical brain maps in the transverse plane are presented to the right of the scatterplots, with highlighted regions in which NDI is reduced with age in bilateral dorsomedial (top) and ventromedial (bottom) frontal cortex. All neuropsychological results account for age, sex, *APOE* ε4 genotype, years of education, and parental history of AD.

Table 1

Characteristics of participants. All values are mean (SD) except where otherwise indicated. Two participants scoring poorly on TMT-B were excluded. AD = Alzheimer's disease; *APOE* ε4 = the varepsilon 4 allele of the apolipoprotein E gene; MMSE = Mini-Mental State Examination; RAVLT = Rey Auditory Verbal Learning Test; TMT = Trail-Making Test.

Sample Characteristics	Ages 45–55	Ages 55–65	Ages 65–75	Total
N	18	59	39	116
Age (years)	52.2 (2.8)	60.2 (3.1)	68.3 (2.1)	61.7 (6.1)
Sex (% Female)	67%	69%	53%	62%
APOE ε4 (% Positive)	22%	45%	43%	40%
AD Parental History (%Positive)	83%	64%	78%	72%
Education (Years)	17.7 (3.1)	16.8 (2.6)	17.0 (2.3)	17.0 (2.7)
MMSE	29.6 (0.7)	29.4 (0.9)	29.0 (1.3)	29.3 (1.0)
RAVLT Immediate Score	7.1 (2.1)	7.1 (2.0)	6.1 (1.5)	6.7 (1.9)
RAVLT Learning Score	48.8 (6.5)	47.4 (6.0)	41.2 (6.4)	45.3 (7.0)
RAVLT Delayed Score	12.4 (2.0)	11.5 (2.5)	9.4 (3.4)	10.8 (3.1)
TMT Part B Score (n=114)	42.6 (9.3)	57.4 (17.6)	74.5 (32.3)	59.0 (20.2)
Days between cognitive testing and MRI	173 (145)	104 (130)	90 (110)	110 (128)

Table 2

Summary of the reductions in neurite density (NDI) in white matter regions, presented in the Montreal Neurological Institute (MNI) coordinate system. FWE = Family-wise error

Peak Cluster MNI Coordinates	Cluster Size (Voxels)	Peak Voxel T-Statistic	Cluster P-value
18 45 −8	198	6.06	0.000
11 13 54	115	5.90	0.000
−20 25 −7	280	5.89	0.000
−32 −9 19	62	5.83	0.000
16 46 16	48	5.71	0.001
13 37 34	48	5.61	0.001
29 −14 13	58	5.57	0.000
−15 30 35	41	5.50	0.001
−32 24 19	26	5.42	0.002
23 29 −3	96	5.25	0.000
−13 48 24	27	5.24	0.002